

## COST-OPTIMIZED METALLIZATION LAYOUT FOR METAL WRAP THROUGH (MWT) SOLAR CELLS AND MODULES

M. Hendrichs, B. Thaidigsmann, T. Fellmeth, S. Nold, A. Spribille, P. Herrmann, M. Mittag, I. Hädrich, U. Eitner, F. Clement, D. Biro, R. Preu

Fraunhofer Institute for Solar Energy Systems ISE, Heidenhofstr. 2, D-79110 Freiburg, Germany

**ABSTRACT:** The cost-effective production of highly efficient solar cells and modules is one of the major goals of current research activities. Especially the ongoing crisis that is affecting a major part of the solar industry makes new methods and instruments for further reductions in cost of ownership (€/Wp) of solar cells and modules essential. Our approach is the optimization of the metallization layout of passivated Czochralski-Si metal wrap through (MWT) solar cells aiming at minimum module cost of ownership. The front finger width, the number of contact rows and the number of solder pads per contact row are varied methodically using analytical modeling. The results of the simulation provide the basis for a bottom-up cost of ownership calculation of MWT solar cells and modules. MWT-metallization layouts with more than four contact rows are identified as most cost-effective. A comparison between MWT and conventional H-pattern technology reveals a cost advantage of over 2 % relative for the MWT approach on module level.

**Keywords:** cost calculation, crystalline silicon solar cell, metallization, MWT

### 1 INTRODUCTION

Back-contact solar cells such as metal wrap through (MWT) solar cells [1] have a huge potential for reaching high conversion efficiencies. Up to date conversion efficiencies over 20 % have been demonstrated for large area p-type Si MWT solar cells using industrial production equipment [2–5]. In comparison to similar H-pattern solar cells the conversion efficiency of the MWT technology is generally increased by around 0.3-0.5 % absolute [6–8]. Nevertheless the high power output of the solar cells comes along with increased costs for cell production and module integration. On cell level the additional production effort of the High-Performance (HIP-MWT) approach (Figure 1a) [7] compared to p-type H-pattern cells with passivated emitter and rear (PERC) [9] (Figure 1b) is reduced to only one process step - namely the drilling of the vias. Up to now there are two industrial MWT module assembly concepts available: A ribbon based [10] and a conductive back sheet based interconnection process [11]. Both module approaches result in very low cell-to-module conversion efficiency losses of  $CTM_{\eta} \approx 1\%$  absolute on aperture area [12–15].

In this contribution we show a method to minimize the cost of ownership of ribbon based HIP-MWT solar modules by varying the cell metallization layout. The presented approach is based on analytical simulations and bottom-up cost calculations. Furthermore a detailed comparison between conventional H-pattern and MWT solar cell and module technology regarding conversion efficiency and cost of ownership is included in this study.

### 2 APPROACH

The metallization layout of p-type HIP-MWT and H-pattern PERC solar cells is varied systematically regarding the number of contact rows, the number of rear contact pads and the front contact finger width using *Gridmaster* [16]. In this simulation tool all contributions to the series resistance  $R_s$  and the dark saturation-currents  $j_{01}$  and  $j_{02}$  are calculated for a given metallization layout using analytical equations. Applying the two diode model the I-V curve is computed enabling the determination of the most important solar cell parameters such as conversion efficiency, fill factor, short-circuit current and

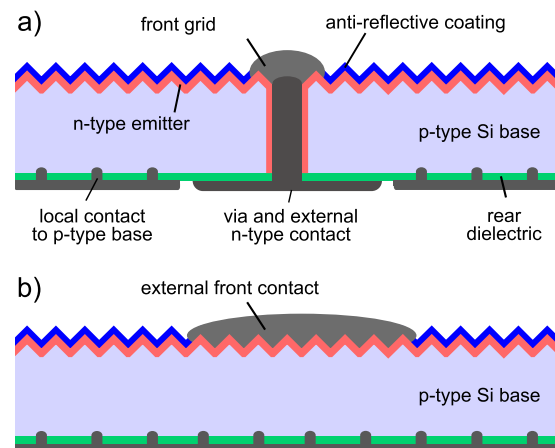


**Figure 1:** Schematic cross section of the p-type HIP-MWT (a) and the H-pattern PERC (b) cell structure investigated in this study.

open-circuit voltage. This allows for the optimization of the number of front contact fingers and the busbar width for a given metallization layout. Furthermore the silver consumption is calculated.

Using the bottom-up cost modeling tool *SCost* [17] the cost of ownership in €/Wp is calculated for all simulated cell metallization layouts. By calculating the cell-to-module conversion efficiency ratio ( $CTM_{\eta}$ ) the resulting module conversion efficiencies are determined for selected cell metallization layouts. For both solar cell technologies the investigated module assembly process is based on conventional tabbing and stringing.

### 3 RESULTS AND DISCUSSION

All investigated p-type HIP-MWT and H-pattern PERC metallization layouts feature rear contact pads with a diameter of 2 mm and constantly five p-type pads per contact row. Exemplary two metallization layouts of HIP-MWT and H-pattern PERC cells with five contact rows are depicted in Figure 2. In case of the MWT solar cells an asymmetrical rear layout with an equal number of n- and p-type contact rows is assumed, as it is typically applied for ribbon interconnected MWT solar cells

[10,18,15]. The front pseudo-busbars are tapered linearly with a minimum busbar width of  $60\ \mu\text{m}$  as shown in Figure 2a.

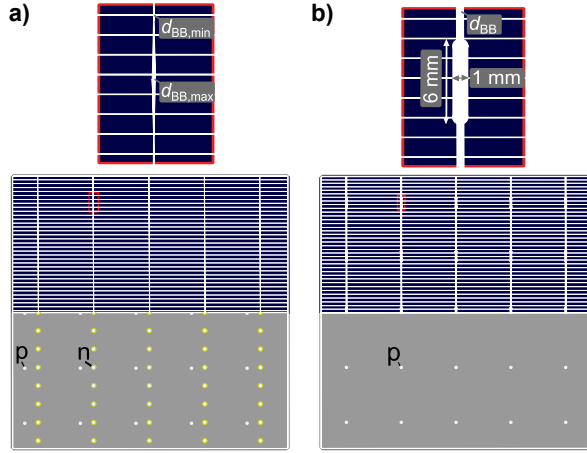


**Figure 2:** Metallization layouts of p-type HIP-MWT (a) and H-pattern PERC (b) solar cells with five contact rows and an edge length of 156 mm. In the amplification the assumed front busbar layouts for both cell technologies are depicted.

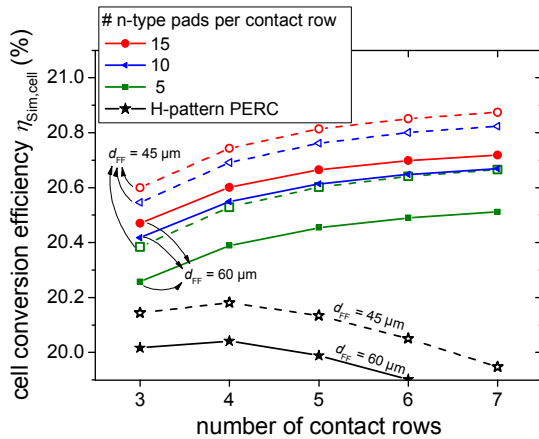


**Figure 3:** Simulated conversion efficiencies  $\eta_{\text{Sim,cell}}$  of 156 mm full-square p-type Cz-Si HIP-MWT and H-pattern PERC solar cells with different metallization layouts and finger widths  $d_{\text{FF}}$ . All data are generated with the analytical simulation tool *Gridmaster*. The front busbar widths of all solar cells are shown in Table II and III. Open (filled) symbols correspond to a finger width of  $d_{\text{FF}} = 45\ \mu\text{m}$  ( $d_{\text{FF}} = 60\ \mu\text{m}$ ).

**Table II:** Optimized maximum busbar width  $d_{\text{BB,max}}$  for all investigated HIP-MWT solar cell metallization layouts.

number of contact rows	number of n-type contact pads per contact row		
	5	10	15
	$d_{\text{BB,max}}$ ( $\mu\text{m}$ )	$d_{\text{BB,max}}$ ( $\mu\text{m}$ )	$d_{\text{BB,max}}$ ( $\mu\text{m}$ )
3	770	370	240
4	570	270	170
5	450	210	130
6	370	170	110
7	310	140	90

The maximum busbar width  $d_{\text{BB,max}}$  is conversion efficiency-optimized for each layout according to the *Gridmaster* simulation, so that all layouts with the same number of n-type pads per contact row feature an equal busbar related series resistance  $R_{\text{S,BB}}$ . The optimized values for  $d_{\text{BB,max}}$  are shown in Table II. On the rear the spacing between aluminum and n-type silver contact pad is  $500\ \mu\text{m}$  for all metallization layouts. The via resistance is  $1\ \text{m}\Omega$  per n-type contact pad. For the H-pattern solar cells the front grid features nonlinearly tapered external front busbars as shown in Figure 2b. The number of the elongated front solder pads is five per contact row and the front busbar width is  $d_{\text{BB}} = 500\ \mu\text{m}$  for all metallization layouts. It is assumed that the H-pattern solar cells are shadowed by a continuous busbar measuring  $1.0\ \text{mm}$  in width for each contact row during I-V measurement. For both cell technologies the number of front contact fingers is conversion efficiency-optimized for all investigated metallization layouts and finger widths according to the *Gridmaster* simulation.

In case of MWT solar cells increasing number of contact rows results in a decrease of  $R_{\text{S,Grid}}$ ,  $R_{\text{S,Via}}$  and  $R_{\text{S,Al}}$  since the current paths in the front contact fingers and in the rear aluminum contact are shortened and the number of vias is increased. This leads to a fill factor gain. In addition the metal covered front surface is reduced with increasing number of contact rows because the optimal number of front contact fingers is lowered. Since the maximum width of the front pseudo-busbars is decreased with every additional contact row (see Table II), the busbar related front metal coverage is equal regardless of the number of contact rows. The overall reduced front metallization leads to reduced shading and front contact related recombinative losses resulting in slightly increased  $J_{\text{SC}}$  and  $V_{\text{OC}}$  values in case of metallization layouts with increased number of contact rows. As a result of the reduction of  $R_{\text{S}}$  and the gain in  $J_{\text{SC}}$  and  $V_{\text{OC}}$  the conversion efficiency is increased by about  $0.2\ \%$  absolute changing the metallization layout from MWT3 to MWT5. Experimentally obtained results presented confirm this trend [19]. The decrease of the front contact finger width from  $60\ \mu\text{m}$  to  $45\ \mu\text{m}$  leads to reduced shading, reduced recombinative losses at the front contact and reduced  $R_{\text{S,Grid}}$  resulting in a conversion efficiency increase of more than  $0.1\ \%$  absolute for metallization layouts with equal number of contact rows and n-type pads. An increased number of n-type contact pads per contact row leads to a reduction of  $R_{\text{S,BB}}$  resulting in higher cell conversion efficiencies. The comparison between H-pattern PERC and HIP-MWT demonstrates that depending on the metallization layout conversion efficiency gains over  $0.6\ \%$  absolute are feasible with the MWT concept.

The bottom-up cost modeling tool *SCost* is used to calculate the cost of ownership of HIP-MWT and H-pattern PERC solar cells with different metallization layouts, see Figure 4. Relying on cost data provided by industrial partners we assume our cost-of-ownership calculation to be representative for an industrial cell production facility with a capacity of 400 MWp per year located in Europe. For the silver paste a price of  $670\ \text{€}/\text{kg}$

is assumed. The costs for the p-type Cz-Si are included with 0.98 €/wafer. For the anti-reflective coating consisting of a silicon nitride as well as the rear passivation consisting of a stack of aluminum oxide [20] and silicon nitride PEVCD processes are calculated. For both cell technologies the simulated process sequence is equal except for the additional laser process in case of the HIP-MWT solar cells.

For the given contact pad size and geometry a HIP-MWT layout with five contact rows is the most cost-effective metallization layout. Increasing the number of contact rows from three to five results in a reduction of the cost of ownership of about 0.2 €/Wp. Furthermore the analysis shows that a metallization layout with more than 10 n-type pads per contact row clearly gains advantages.

On cell level the HIP-MWT technology is already more cost-effective than the H-pattern PERC concept. The question is whether the cost of ownership advantage of the HIP-MWT solar cells can be transferred to the module level.

In this study we investigate an MWT module concept based on a modified tabbing and stringing process [10,18,15]. The rear pad insulation is realized by an isolation layer that is applied during the adapted tabbing and stringing process. Table IV shows the assumed ribbon dimensions for the simulated 60 cell HIP-MWT and H-pattern PERC solar modules.

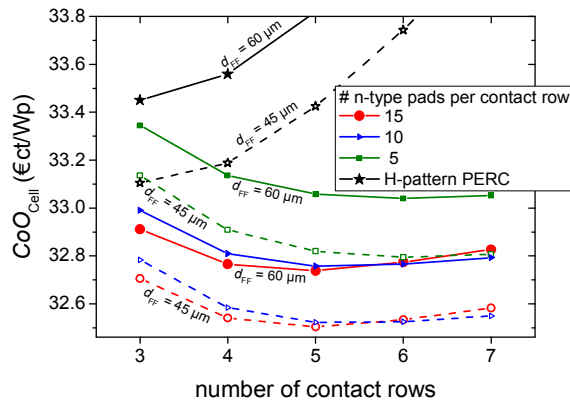


**Figure 4:** Calculated cost of ownership  $CoO_{Cell}$  of 156 mm full-square p-type Cz-Si HIP-MWT and H-pattern PERC solar cells with different metallization layouts and finger widths  $d_{FF}$ . All data are based on the simulated cell conversion efficiencies shown in Figure 3. Open (filled) symbols correspond to a finger width of  $d_{FF} = 45 \mu\text{m}$  ( $d_{FF} = 60 \mu\text{m}$ ).

**Table IV:** Ribbon dimensions for HIP-MWT and H-pattern PERC 60 cell solar modules with different metallization layouts.

number of contact rows	ribbon width / ribbon thickness (mm / $\mu\text{m}$ )	
	HIP-MWT	H-pattern PERC
3	4.0 / 200	1.5 / 180
4	4.0 / 150	1.2 / 170
5	4.0 / 120	1.0 / 160
6	4.0 / 100	1.0 / 135
7	4.0 / 85	1.0 / 120

**Table V:** Relative conversion efficiency ratio  $CTM_{\eta,electr.}$  caused by resistive losses in cell and string interconnectors and solder joints for HIP-MWT and H-pattern PERC 60 cell solar modules with different metallization layouts. The analyzed HIP-MWT metallization layouts feature 15 n-type pads per contact row.

number of contact rows	$CTM_{\eta,electr.}$ (%)	
	HIP-MWT	H-pattern PERC
3	-1.5	-3.8
4	-1.4	-3.7
5	-1.4	-3.7
6	-1.3	-3.7
7	-1.3	-3.6

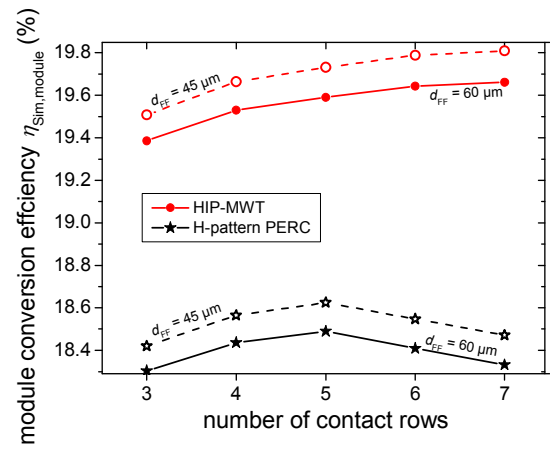


**Figure 5:** Simulated conversion efficiencies  $\eta_{Sim,module}$  of 60 cell p-type Cz-Si HIP-MWT and H-pattern PERC solar modules with different metallization layouts and finger widths  $d_{FF}$ . The corresponding cell conversion efficiencies are shown in Figure 3. The HIP-MWT solar cells feature 15 n-type pads per contact row. Open (filled) symbols correspond to a finger width of  $d_{FF} = 45 \mu\text{m}$  ( $d_{FF} = 60 \mu\text{m}$ ).

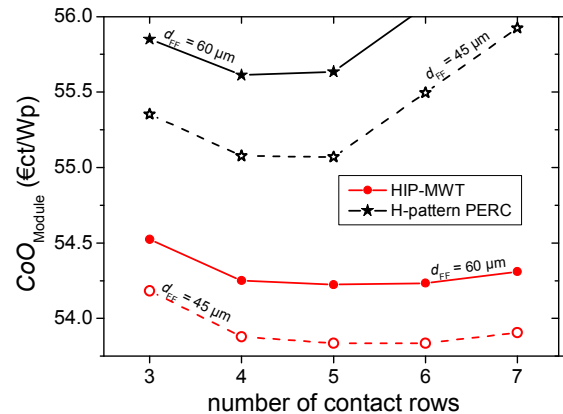


**Figure 6:** Calculated cost of ownership  $CoO_{Module}$  of p-type Cz-Si HIP-MWT and H-pattern PERC solar modules with different metallization layouts and finger widths  $d_{FF}$ . All data are based on the simulated module conversion efficiencies shown in Figure 5. The HIP-MWT solar cells feature 15 n-type pads per contact row. Open (filled) symbols correspond to a finger width of  $d_{FF} = 45 \mu\text{m}$  ( $d_{FF} = 60 \mu\text{m}$ ).

For both cell technologies the simulated module conversion efficiencies are related to the module aperture area with an assumed cell and edge gap of 2 mm. For 156 mm full-square solar cells this results in a  $CTM_{\eta}$  of -2.8 % relative due to the inactive module area for all simulated solar module efficiencies. Optical losses and gains caused by the various interactions between cell, encapsulant, back sheet and glass are assumed to sum-up in an optical  $CTM_{\eta}$  of -1.0 % relative. The influence of the coupling gain generated by light coupling of the cell front metallization is neglected in this study. Furthermore mismatch losses are not taken into account neither for the HIP-MWT nor for the H-pattern PERC modules. The CTM resulting from electrical losses in the cell and string interconnectors and solder joints is calculated for all ribbon dimensions (see Table IV) and metallization layouts using analytical simulation. The basis for the calculation is the cell current at the point of maximum power that is applied into the ribbon along the contact pad area. For the determination of contact resistive losses at the solder joint an experimentally obtained value of  $35 \mu\Omega\text{cm}^2$  is used. The results for  $CTM_{\eta,electr.}$  are shown in Table V.

Figure 5 shows the simulated conversion efficiencies for 60 cell HIP-MWT and H-pattern PERC solar modules. As well as on cell level the module conversion efficiency gain of the MWT5 layout is up to 0.2 % absolute in comparison to the MWT3 layout. The conversion efficiency advantage of the HIP-MWT technology compared to the conventional H-pattern approach is increased on module level and amounts to 1 % absolute for metallization layouts with five contact rows. This is mainly due to reduced electrical losses in the cell interconnectors.

In order to evaluate the impact of the metallization layout on the solar module cost of ownership a detailed analysis is carried out using  $SCost$ , see Figure 6. As a basis a standard module assembly consisting of glass, encapsulant, copper ribbons, back sheet, frame and junction box is assumed. The capital and operational expenditures are cost out for a 400 MWp production facility located in Europe. The ribbon costs are calculated according to the metallization layout dependent dimensions (see Table IV) with an expected price of 20 €/kg. Note that no additional costs are assumed for layouts with increased number of solder pads, since no additional material is consumed at the soldering points. In case of the HIP-MWT modules the costs for the isolation layer are included with a price of 3 €/m<sup>2</sup>. It is assumed that the investment for the adapted back-contact tabber-stringer amounts to 125% of a standard tabber-stringer. Again, we find MWT5 to be the most cost-effective metallization layout on module level. For the investigated module assembly process HIP-MWT modules turn out to be more cost-effective than conventional H-pattern PERC modules. The cost advantage of the HIP-MWT technology amounts to over 2 % relative comparing metallization layouts with five contact rows.

#### 4 CONCLUSION

A method for the systematical optimization of the metallization layout of p-type MWT solar cells based on analytical simulation is presented. The target is the reduction of the cost of ownership of MWT solar

modules based on an adapted tabbing and stringing process. Therefore the number of contact rows, the number of n-type pads per contact row and the front contact finger width of HIP-MWT solar cells are varied methodically. For the presumed production technologies, cost data and cell-to-module losses the cost-optimum of HIP-MWT modules is found for cell metallization layouts with more than four contact rows and more than 10 n-type pads per contact row. The comparison between HIP-MWT and conventional H-pattern PERC solar technology reveals a cost advantage of more than 2 % relative for the MWT approach.

#### ACKNOWLEDGEMENTS

The authors thank the Photovoltaic Technology for their support as well as S. Kaufmann from Komax Solar for fruitful discussions. The work was supported by the German Federal Ministry for the Environment, Nature Conservation and Nuclear Safety under contract number 0325491 "Thesso" and by the FhG internal programs under Grant No. WISA 823 236.

#### REFERENCES

- [1] E. van Kerschaver, R. Einhaus, J. Szlufcik et al., "A novel silicon solar cell structure with both external polarity contacts on the back surface", *Proc. 2nd World Conference on Photovoltaic Energy Conversion*, pp. 1479–1482, 1998.
- [2] E. Lohmüller, B. Thaidigsmann, M. Pospischil et al., "20% Efficient Passivated Large-Area Metal Wrap Through Solar Cells on Boron-Doped Cz Silicon", *IEEE Electron Device Lett.*, Vol. 32, No. 12, pp. 1719–1721, 2011.
- [3] B. Thaidigsmann, M. Linse, A. Wolf et al., "The Path to Industrial Production of Highly Efficient Metal Wrap Through Silicon Solar Cells", *GREEN*, Vol. 2, No. 4, pp. 171–176, 2012.
- [4] Canadian Solar", *press release*, 2012.
- [5] B. Thaidigsmann, E. Lohmüller, U. Jäger et al., "Large-area p-type HIP-MWT silicon solar cells with screen printed contacts exceeding 20% efficiency", *Phys. Status Solidi RRL*, Vol. 5, No. 8, pp. 286–288, 2011.
- [6] K. Meyer, H.-J. Krokoszinski, D. Lahmer et al., "Novel MWT cell design on monocrystalline silicon wafers", *Proc. 25th EU PVSEC*, pp. 1774–1777, 2010.
- [7] B. Thaidigsmann, A. Spribille, H. Plagwitz et al., "HIP-MWT – a new cell concept for industrial processing of high-performance metal wrap through silicon solar cells", *Proc. 26th EU PVSEC*, pp. 817–820, 2011.
- [8] F. Clement, M. Menkoe, R. Hoenig et al., "Pilot-line processing of screen-printed CZ-Si MWT solar cells exceeding 17% efficiency", *Proc. 34th IEEE PVSC*, pp. 1–4, 2009.
- [9] A. W. Blakers, A. Wang, A. M. Milne et al., "22.8% efficient silicon solar cell", *Applied Physics Letters*, No. 55, pp. 1363–1365, 1989.
- [10] U. Eitner, D. Eberlein, M. Tranitz, "Interconnector based module technology for thin MWT cells", *Proc. 27th EU PVSEC*, pp. 3461–3464, 2012.
- [11] M. Spaeth, P. de Jong, I. J. Bennett et al., "First experiments on module assembly line using back-

- contact solar cells", *Proc. 23th EU PVSEC*, pp. 2917–2921, 2008.
- [12] M. Lamers, C. Tjengdrawira, M. Koppes et al., "17.9% back-contacted mc-Si cells resulting in module efficiency of 17.0%", *Proc. 25th EU PVSEC*, pp. 1417–1421, 2010.
- [13] H.-H. Hsieh, W.-K. Lee, F.-M. Lin et al., "Performance of metal wrapped through solar module", *Proc. of the 35th IEEE Photovoltaic Specialists Conference*, pp. 2823–2826, 2010.
- [14] I. Hädrich, M. Wiese, B. Thaidigsmann et al., "Minimizing the Optical Cell-to-module Losses for MWT-modules", *Energy Procedia*, No. 38, pp. 355–361, 2013.
- [15] A. Spribille, M. Hendrichs, B. Thaidigsmann et al., "HIP-MWT: Our Approach for High Performance Ribbon Based Back Contact MWT Modules with low CTM Losses", *Proc. 7th SNEC*, 2013.
- [16] T. Fellmeth, F. Clement, D. Biro, "Analytical Modeling of Silicon Solar Cells", *Journal of Photovoltaics*, 10.1109/JPHOTOV.2013.2281105, 2013.
- [17] S. Nold, N. Voigt, L. Friedrich et al., "Cost Modelling of Silicon Solar Cell Production Innovation Along the PV Value Chain", *Proc. 27th EU PVSEC*, pp. 1084–1090, 2012.
- [18] A. Drews, F. Clement, A. Spribille, "HIP-MWT Solar Cells – Pilot-Line Cell Processing and Module Integration", *Proc. 27th EU PVSEC*, pp. 828–831, 2012.
- [19] M. Hendrichs, B. Thaidigsmann, E. Lohmüller et al., "Advanced metallization concepts for p-type silicon MWT solar cells", *Energy Technology*, 10.1002/ente.201300094, 2013.
- [20] P. Saint-Cast, D. Kania, M. Hofmann et al., "Very low surface recombination velocity on p-type c-Si by high-rate plasma-deposited aluminum oxide", *Appl. Phys. Lett.*, Vol. 95, No. 15, p. 151502, 2009.